Fabrication of (U,Ce)O_2 and (U,Am)O_2 pellets with controlled porosity from oxide microspheres

L. Ramond, P. Coste, M. Bataille, S. Picart, A. Gauthe

Fabrication of $(U,Ce)O_2$ and $(U,Am)O_2$ pellets with controlled porosity from oxide microspheres

Laure Ramond*[1], Philippe Coste [1], Marc Bataille[1], Sébastien Picart[2] and Aurélie Gauthé[2]
[1]DEN/DTEC/SECA/LFC
[2]DEN/DRCP/SERA/LCAR
CEA MARCOULE - 30207 Bagnols-sur-Cèze, FRANCE

Abstract

$U_{1-x}Am_xO_{2\pm\delta}$ mixed-oxides are considered as promising compounds for americium heterogeneous transmutation in Sodium Fast Neutron Reactor [1–3]. Comparison between dense (95% of the theoretical density (TD)) and porous (88% TD) oxide microstructure in terms of behavior during irradiation is currently under study through experimental irradiation test [3,4]. Porous microstructure is envisaged in order to facilitate helium and fission gas release and to reduce pellet swelling during irradiation and under self-irradiation.

In this study, we focus on determining the experimental parameters necessary to the fabrication of porous ceramic pellets with controlled porosity (8-10% open porosity) from mixed-oxide microspheres obtained by the Weak Acid Resin (WAR) process [5]. More precisely, uranium-cerium mixed-oxide microspheres were first synthesized by co-loading uranyl and cerium cations onto carboxylic resin beads, Ce being used as a surrogate of Am. Calcination under air of these metal loaded spheres led to the mineralization of the organic matter and to the formation of $(U,Ce)_3O_8$ microspheres. The major part of this as-treated spherules was then submitted to a second thermal treatment under reductive atmosphere (Ar/4vol.%H_2) to form the $(U,Ce)O_2$ solid solution. The specific mix of $(U,Ce)O_2$ and $(U,Ce)_3O_8$ microspheres allowed to obtain, after pelletization and reductive sintering, an optimized porous microstructure, as previously reported by E. Rémy et al. for simple uranium dioxide [6]. Indeed, the reduction of $(U,Ce)_3O_8$ into $(U,Ce)O_2$ during the sintering treatment is accompanied by the formation of open porosity, mainly due to a 3% decrease of the lattice volume and to an oxygen release in the form of H_2O. Porous pellets (D~88% TD), with an open porosity of about 8% were thus fabricated.

Parameters found for $(U,Ce)O_2$ were successfully applied to the fabrication of the highly active $(U_{0.90}Am_{0.10})O_2$ pellets. Finally, an $(U_{0.90}Am_{0.10})O_2$ pellet with controlled porosity of 89% TD was fabricated to demonstrate the scientific feasibility of this spherule metallurgy process.

Introduction

Even though neptunium, americium and curium, known as the minor actinides (MA) represent less than 0.1 wt.% of the spent nuclear fuel, they are the main responsible for long-term radioactivity and heat load of the ultimate waste after plutonium recycling [7,8]. A possible option to reduce the long-term radiotoxicity of spent fuel nuclear wastes is to deploy MA transmutation into lighter short-lived elements, for instance in Fast Neutron Reactors (FNRs) developed in the framework of GEN-IV International Forum [1,9]. The program specially focuses on the transmutation of americium since this element is the most abundant and the most active among MA [2,10]. In France, among the different MA transmutation modes [2,11-13], heterogeneous transmutation is one of the most considered options for the future nuclear fuel cycle [1]. It consists in irradiating uranium–americium mixed-oxide compounds ($U_{1-x}Am_xO_{2\pm\delta}$) located at the core periphery. Such irradiation targets are called AmBB (Americium Bearing Blankets) [3]. The content of americium [Am/(Am+U)] in such materials can reach 15 at.%. In this context, several processes are being developed to fabricate such mixed-oxide pellets which are to meet the specifications required to perform analytical irradiations such as Am content, O/M ratio (oxygen to metal with M = U + Am), chemical and microstructural homogeneity, pellet dimensions and density, open porosity ratio, etc [2,10,14,15].

The development of a dustless innovative route, adapted from the Weak Acid Resin process (WAR) is currently studied. It consists in impregnating resin microspheres with the desired element(s) in their cationic form and then in submitting the metal loaded resin to a calcination step to obtain the single or mixed-oxide microsphere precursors. Those microspheres are then shaped into pellets which are sintered to produce single or mixed-oxide ceramic. The over-all process is the so called Calcined Resin Microsphere Pelletizing (CRMP) process [14].

The fabrication of dense pellets by CRMP process was demonstrated for compounds such as UO_2 [16] and $(U,Am)O_2$ [17]. Tailored-porous samples from oxide spheres were fabricated only for UO_2 [6]. As the main objective of MARIOS and DIAMINO irradiations was to assess the influence of the fuel microstructure (dense and porous), it could be important to also demonstrate the feasibility of $(U,Am)O_2$ pellets fabrication with controlled density from CRMP process for an eventual future irradiation. Indeed, the porous microstructure is considered to facilitate the release of helium produced during irradiation but also to limit pellet swelling under self-irradiation.

In this study, we focus on determining the experimental parameters necessary to the fabrication of porous ceramic pellets with controlled porosity (8-10% open porosity) from mixed-oxide microspheres obtained by the Weak Acid Resin (WAR) process [5]. Firstly, $(U,Ce)O_2$ porous pellets (D~88% TD), with an open porosity of about 8% were fabricated. Secondly, experimental parameters found for $(U,Ce)O_2$ were applied to the fabrication of the highly active $(U_{0.90}Am_{0.10})O_2$ pellets. Finally, an $(U_{0.90}Am_{0.10})O_2$ pellet with controlled porosity (89%TD) and with an open porosity of 9% was fabricated.

Fabrication of $(U,Ce)O_2$ pellets with controlled porosity

Resin preparation

The ion exchange resin used for the fixation was an IMAC HP333 carboxylic resin supplied by Dow Chemicals (Chauny, France). The resin was manually sieved under deionised water and the 630-800 µm diameter size range was collected for the fixation. The resin was introduced in a column to be washed by successive percolations of 1 M nitric acid (HNO_3 - Fisher Chemical, Certified ACS Plus), demineralized water, 1 M ammonia solution (Merck, Pro Analysis) and demineralized water again. Eventually, the washed resin was prepared in its protonated form by a final percolation of 1 M HNO_3, followed by a demineralized water rinse cycle.

Preparation of the loading solution (U/Ce)

As the fixation of cerium on the resin is not congruent, a content of [Ce/(U+Ce)] = 25 at.% in the solution was selected in order to obtain 15 at.% Ce in the resin [16].

The loading solution was prepared by first dissolving 64 g of cerium (III) nitrate hexahydrate ($Ce(NO_3)_3,6H_2O$ - 99.99% Sigma Aldrich) in a 0.347 M HNO_3 solution (volume = 1.65L). Then uranium trioxide solid (UO_3) was added to this solution. The latter was an Acid Deficient Uranyle Nitrate solution (ADUN) [18]. After 12h stirring, the solution was filtered to remove UO_3 excess. The final concentration of uranium and cerium was 270 mmol and 89 mmol, respectively, which corresponds to a Ce/(Ce+U) ratio of 24,8%, and the pH value was 3.3.

Impregnation

Resin beads were introduced in a glass chromatography column (2.5 cm diameter and 30 cm height - Biorad). Fixation of both UO_2^{2+} and Ce^{3+} cations was performed by percolating the ADUN solution by recirculation through the column during 6 h. The loaded resin was rinsed with demineralized water before being dried at 105°C overnight in an air oven. 50 g of dried loaded resin were prepared in one go.

In order to measure the amount of metal cations fixed by the resin, a sample of 150 mg of dried metal loaded microspheres was contacted with 5 mL of 1 M HNO_3 in a column for 1h and then rinsed 4 times with same amount of acid. All fractions were collected in a 25 mL jauged flask and the obtained solution was finally analyzed by inductively coupled plasma-atomic emission spectroscopy (ICP-AES). The cerium content versus total metal content [Ce/(Ce+U)] on the loaded resin microspheres was determined to be equal to 13.8 at.% which is closed to the targeted 15 at.%.

Calcination - Heat treatment

Two thermal treatments were then applied to the loaded resin in an instrumented tubular furnace.

The resin was first calcined at 700°C for 4h under air (flow 600 $L.h^{-1}$) with a low heating rate of 1.5$K.min^{-1}$preventing any microsphere degradation and guarantying a proper homogeneity of the calcination temperature. A part of the latter was then submitted to a second heat treatment under reductive atmosphere Ar/4vol.%H_2 (flow 600 $L.h^{-1}$) at 700°C for 5h with a heating rate of 10 $K.min^{-1}$.

In terms of mass loss, total weight loss of 56.2% and 4.2% was observed during the first and second thermal cycle, respectively. Those values are consistent with values generally encountered for uranium loaded resin bead [6,14].

Figure 1: Microspheres a) before calcination under air (total weight~50g) b) after calcination under air 700°C-4h (total weight~22g)

a) 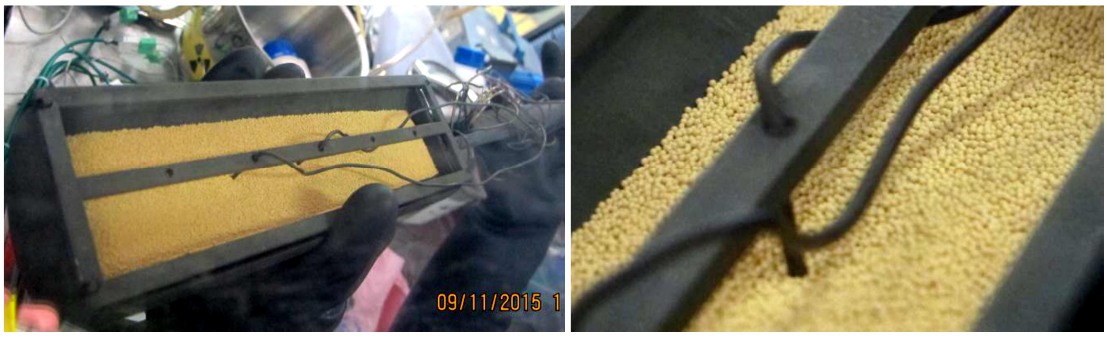

b) 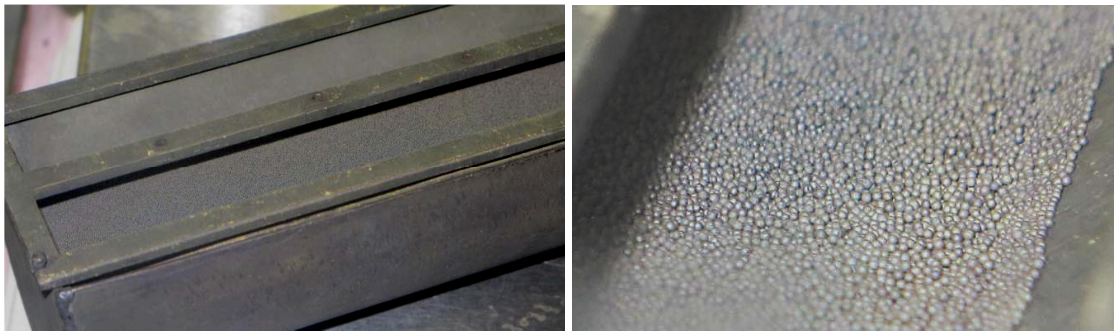

Oxide microsphere characterization

Crystalline structure analyses on the obtained microspheres were performed by X-ray diffraction (XRD) using a Bruker D8 Advance diffractometer (Madison, WI) with a Cu X-ray source (Kα1/α2, λ = 1.54059/1.54439 Å) and equipped with a special sample holder for radioactive material measurements. The microspheres were first milled manually and then mixed in grease with Au powder (Sigma Aldrich, >99.9%). Gold is used as standard to control any potential instrumental deviation.

The XRD patterns obtained from the powdered oxide microsphere after calcination under air and after reduction in Ar/4vol.%$H_2$are presented in Figure 2 in red (bottom) and blue (top), respectively.

Figure 2: XRD patterns for microspheres after the first calcination (air), and after second heat treatment (Ar/4%H_2) (*gold standard)

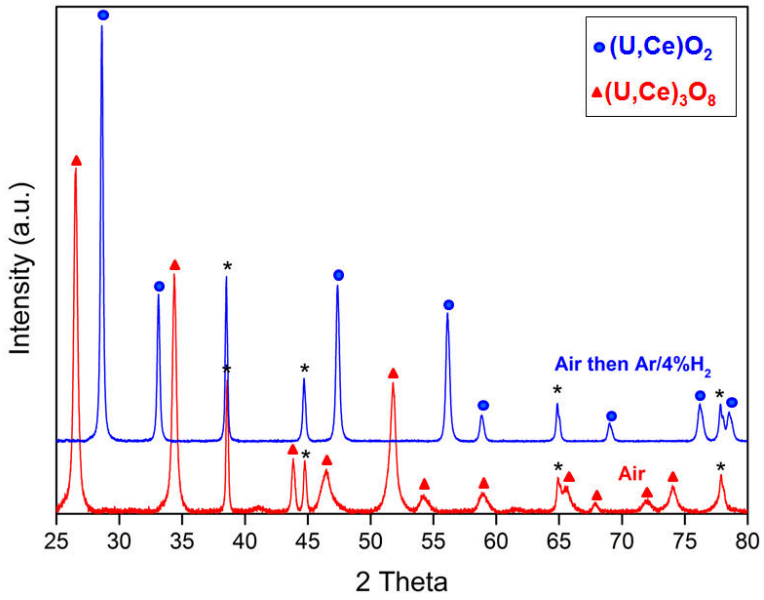

After the calcination under air, the XRD pattern is characteristic of a single hexagonal phase (P-62m) with the following refined parameters, a=6.811 (1) Å and c=4.161 (1) Å.

After the reduction step under Ar/4vol.%H_2, only peaks derived of a single fluorite-type phase (Fm-3m) are visible. The refined lattice parameter was found equal to 5.459 (1) Å. No trace of the $(U,Ce)_3O_8$ hexagonal phase is revealed which proves the total reduction of $(U,Ce)_3O_8$ to $(U,Ce)O_2$.

A nuclearized ZEISS Supra 55 VP Field Emission Gun (FEG) scanning electron microscopy (SEM (Oberkochen, Germany) was used for the morphology and the microstructure observations of the oxide microspheres. SEM observation (Figure 3) revealed that the spheres have a porous microstructure after calcination under air as well as after the second heat treatment under Ar/4vol.%H_2. Energy dispersive spectroscopy revealed homogeneity of U and Ce distributions between microspheres.

Figure 3: FEG-SEM micrographs in secondary electron mode of oxide microspheres: (a) $(U,Ce)_3O_8$ and (b) $(U,Ce)O_2$

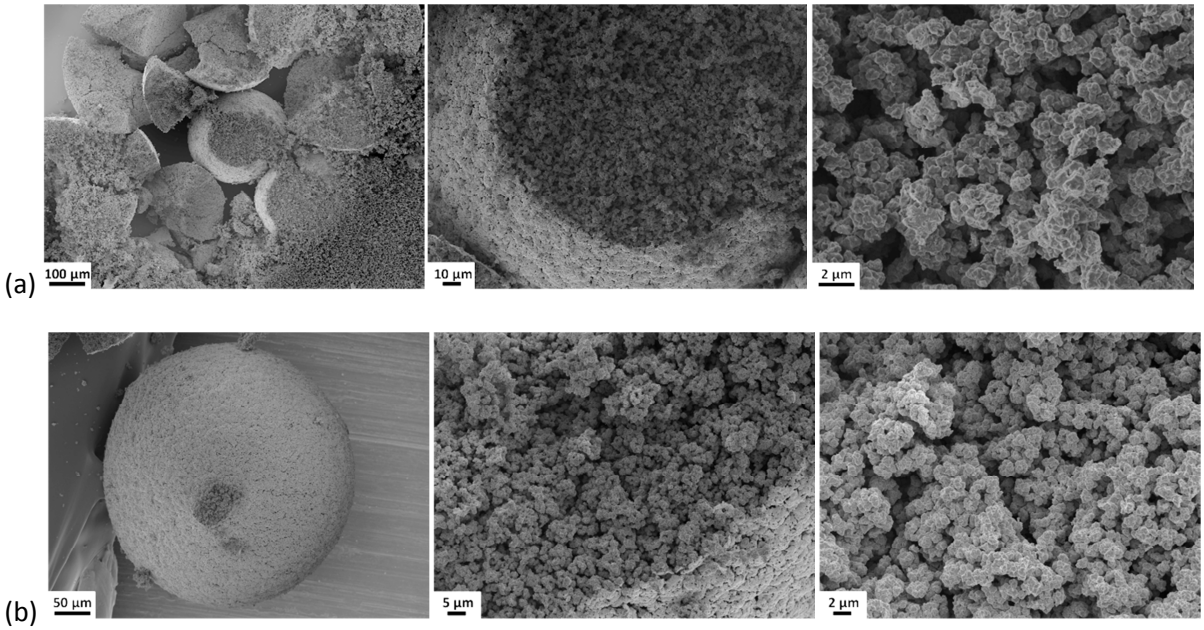

Fabrication and characterization of U-Ce mixed-oxide pellets with controlled porosity

To fabricate porous pellets, reduced microspheres $(U,Ce)O_2$ were mixed with oxidized microspheres $(U,Ce)_3O_8$ (Figure 4). Different contents of oxidized spheres (30, 35 and 40 wt.%) were used in order to obtain samples with a density in the 86-90% TD range, with a homogeneous open porosity network. After the pelletization step in a three-part matrix (5.0 mm diameter) , the green pellets (about 500 mg each) were sintered under reductive atmosphere at 1850°C-5min in a horizontal dilatometer or at 1700°C-4h in a high temperature furnace.

XRD diffractograms obtained on the sintered pellets are presented in figure 5. These patterns are characteristic of the fluorite-type phase, with a refined parameter of 5.462(1), 5.463(1) and 5.464(1) Å, for a $(U,Ce)_3O_8$ content of 30, 35 and 40wt.%, respectively. The sintering step under Ar/4vol.%H_2 ensured the total reduction of $(U,Ce)_3O_8$ to $(U,Ce)O_2$, with a volume lattice decrease from an hexagonal to a fluorite phase.

Figure 4: Porous pellets fabrication flowchart using oxide microsphere precursors

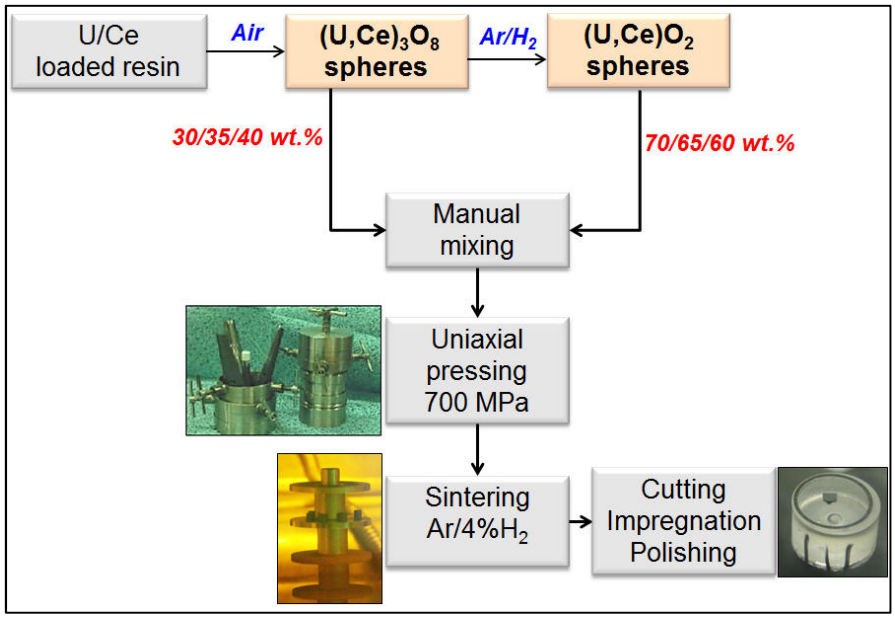

Figure 5: XRD patterns of sintered pellets (1850°C-5min) for different $(U,Ce)_3O_8/(U,Ce)O_2$ ratios *(*gold standard)*

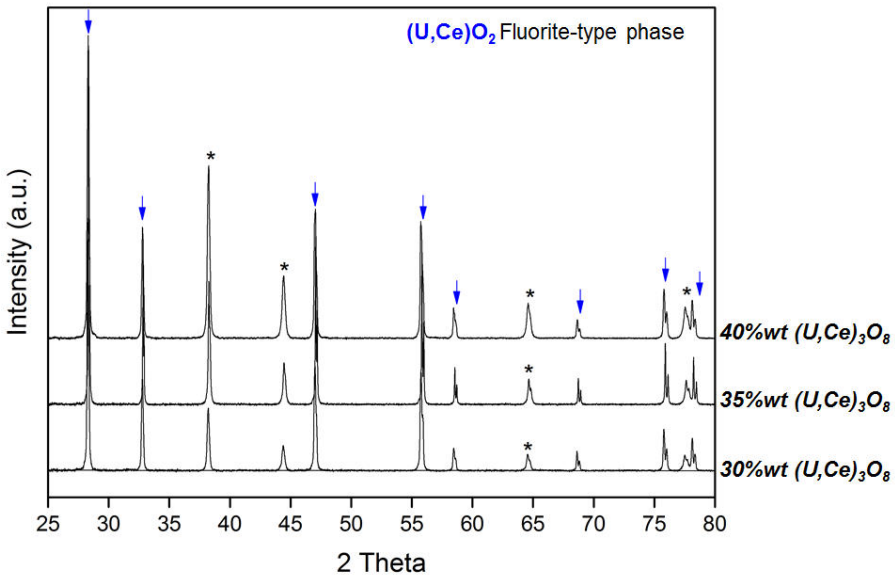

Sintered pellets were cut longitudinally then mirror-polished before being observed with an optical video microscope (Olympus BX 30). Figure 6 presents the microstructure of pellets sintered at 1850°C-5min, for 30, 35 and 40 wt.% of $(U,Ce)_3O_8$. The observations clearly exhibit the porous

microstructure of these samples which have a density between 86 and 89% TD (the final density of each sintered sample was obtained via the Archimedes method using de-ionized water as the immersion medium). The percolating porosity network was created during the reductive sintering by volume shrinkage of $(U,Ce)_3O_8$ phase in $(U,Ce)O_2$. The results for 30 and 35 wt.% are quite similar; the open porosity is about 8%. A significant difference can be observed for the 40 wt.% sample where the open porosity reaches 10%. This high ratio of porosity induced a lower mechanical resistance and grains removal during polishing as observed. To insure good mechanical resistance while keeping a correct ratio of open porosity (≥ 8%), a content of 30-35 wt.% will be selected for the next fabrications, and in particular for the fabrication of porous $(U,Am)O_2$.

Figure 6: Optical microscopic observations of the internal microstructure of sintered pellets

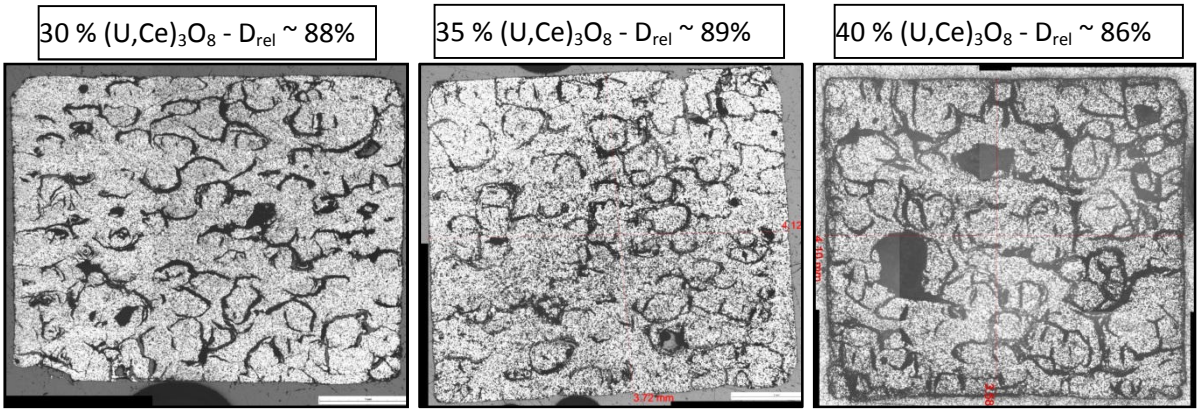

Fabrication of $(U,Am)O_2$ pellet with controlled porosity

Uranium-americium mixed oxide microsphere synthesis

The microspheres used for the fabrication of the pellet were synthesized according to previously published procedure [14]. The resin preparation was the same than described in first section for U/Ce (sieving of resin bead in the 630-800 µm size range, extensive washing cycle, resin prepared in its protonated form).

The resin microspheres were impregnated by an acid deficient nitrate uranyle solution (ADUN) mixed to americium (III) nitrate (with a concentration of americium [Am/(Am+U)]= 10.1 ± 0.2 at.%) during 5h by recirculation through a plexiglass column. After drying, the microspheres were first calcined in air at 700°C for 4h. A part of these oxide microspheres was secondly reduced in Ar/4vol.%H_2 at 700°C for 5h (same heat treatment parameters than $(U,Ce)O_2$).

Figure 7: Pictures of U-Am oxide microspheres synthesis in hot cell in Atalante facility. From left to right: loaded resin in plexiglass column, loaded resin in the quartz crucible before calcination in airflow and oxidized $(U,Am)_3O_8$ microspheres

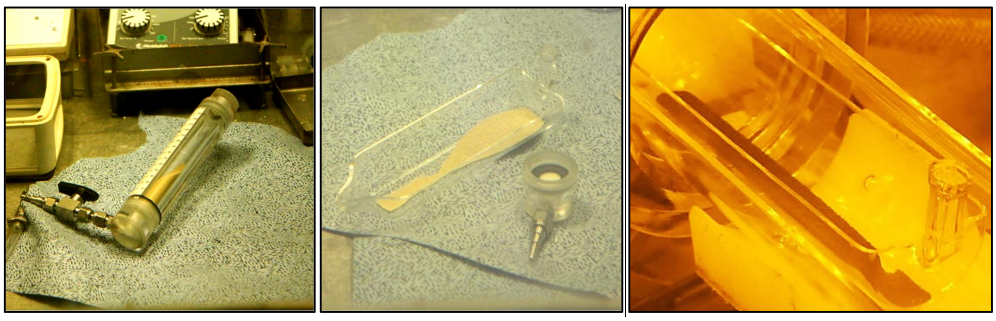

Characterization of U-Am mixed-oxide microspheres

A content of 11.1 ±0.2 at.% Am measured by TIMS analysis by dissolving 20 mg of reduced oxide microspheres $(U,Am)O_2$ in nitric acid (5 M), which can demonstrate the quasi-congruence of the Am fixation (~10 at.% in the initial solution).

The XRD patterns obtained from the powdered oxide microsphere after calcination under air and followed by a reduction step under Ar/4vol.%H_2 are presented in Figure 8 in red (bottom) and blue (top), respectively.

After the calcination under air, the XRD pattern is characteristic of a single hexagonal phase (P-62m) with the following refined parameters a=6.838 (1) Å and c=4.165 (1) Å.

After the reduction under Ar/4vol.%H_2, only peaks derived of a single fluorite-type phase (Fm-3m) are visible which proves the quantitative reduction of $(U,Am)_3O_8$ to $(U,Am)O_2$. The refined lattice parameter was found equal to 5.467 (1) Å. This parameter is higher than the one previously obtained by E. Remy et al. [17] (5.4511 Å) with the same CRMP process, which indicates a higher reduction for our sample.

Figure 8: XRD patterns for U-Am oxide microspheres after the first calcination (air, at the bottom), and after second heat treatment (Ar/4vol.%H_2) (*gold standard)

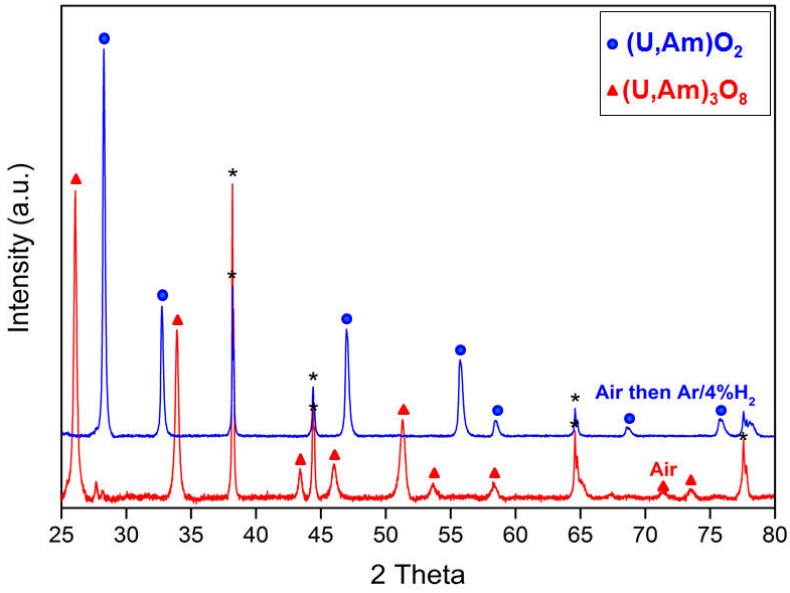

Fabrication and characterization of U-Am mixed-oxide pellet with controlled porosity

The ultimate goal of this study was to demonstrate the fabrication of a porous AmBB pellet (86-90% TD) with an open porosity higher than 8% (expected specifications for AmBB porous pellets). The same process presented in Figure 4 was used for the fabrication of porous $(U,Am)O_2$.

A proportion of 65 wt.% of reduced microspheres $(U,Am)O_2$ were mixed with 35 wt.% of oxidized $(U,Am)_3O_8$ microspheres. This ratio of 65/35 was chosen in order to get the specified density (about 88% TD) while keeping a sufficient mechanical resistance of the sintered pellet. After a pelletization step at 700 MPa, the green pellet was sintered at 1700°C-4h under reductive atmosphere (Ar/4vol.%H_2). After sintering, the final pellet (m=560 mg, h=4.4mm, diameter =4.1mm) is rectilinear and neither deformations nor particular defects were observed.

The final density was obtained via the Archimedes method in deionized water. It was found a density of 89% TD with 9% of open porosity and 2% of closed porosity. These characteristics strongly fit with the required porous pellet specifications for previous irradiation programs such as MARIOS [19,21].

Figure 9 presents a longitudinal observation of the sintered $(U,Am)O_2$ pellet by optical microscopy. The porosity is homogeneously distributed through the pellet and the open porosity is interconnected. Memory form of ex-$(U,Am)_3O_8$ microspheres is rather hemispherical and could be compared with the memory form of ex-U_3O_8-AmO_2 agglomerates observed in MARIOS samples which had no specific form.

XRD pattern obtained on the sintered pellet is characteristic of the fluorite-type phase, with a refined parameter of 5.470 (1) Å. The latter is very close to usual lattice parameter found for $U_{0.90}Am_{0.10}O_{2\pm\delta}$ sintered pellets fabricated by metallurgical process [19,20]. The sintering step provided the total reduction of $(U,Am)_3O_8$ to $(U,Am)O_2$, with a volume lattice decrease for an hexagonal to a fluorite phase creating the visible open porosity network (Figure 9).

Figure 9: Optical microscopic observation of the internal microstructure of sintered $(U,Am)O_2$ porous pellet

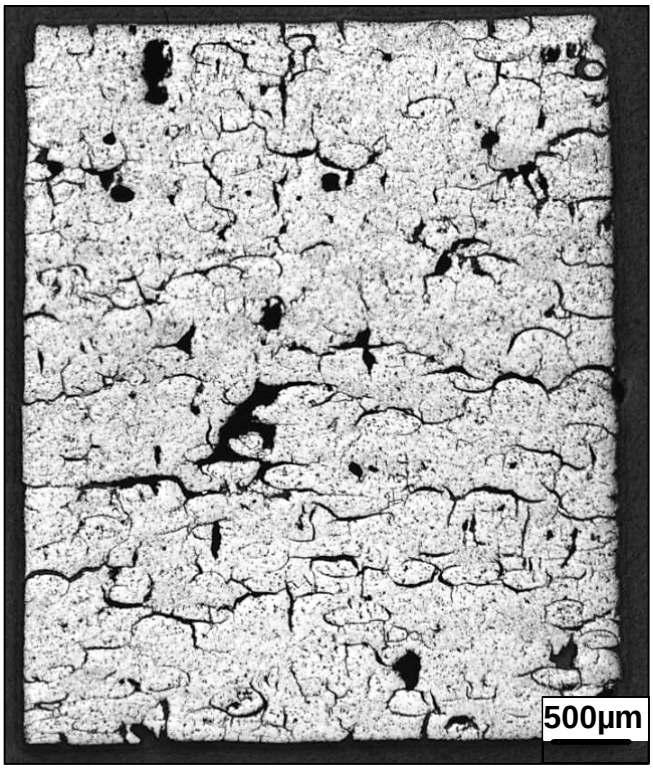

Conclusion

This work focussed on the fabrication of mixed-oxide pellets with controlled porosity by implementing the CRMP process. The synthesis of mixed-oxide microspheres by impregnation and calcination of loaded resin beads really limits the production of fine particles. Moreover, the CRMP process is a simplified one, with only two steps after the oxide microsphere synthesis: pelletizing and sintering. The feasibility of porous AmBB fabrication was demonstrated for a potential heterogeneous transmutation of americium in FNRs by the fabrication of an 89% DT porous pellet with 9% of open porosity. The developed process allows a homogeneous distribution of the open porosity through the entire pellet created by the complete reduction of hexagonal $(U,Am)_3O_8$ into fluorite-type phase $(U,Am)O_2$.

This porosity network could be tuned by modifying the initial resin bead diameter or by doing a specific mix between several microsphere diameters.

Acknowledgements

The authors are thankful to P. Grangaud, J.M. Pomarède, Y. Sinot for uranium-americium mixed oxide microsphere synthesis, N. Bousquet, A. Achabouni for the calcination of $(U,Ce)O_2$ spherules, E. Pascal for optical microscopy, J.R. Sevilla for SEM observations, R. Vauchy and A. Joly for XRD on sintered $(U,Am)O_2$. The authors also acknowledge the CEA PACFA program for financial support.

References

[1] D. Warin (2007), "Status of the French Research Program on Partitioning and Transmutation", J. Nucl. Sci. Technol., 44 , pp. 410–414.

[2] D. Prieur et al. (2011), "Fabrication and characterisation of $U_{0.85}Am_{0.15}O_{2-x}$ discs for MARIOS irradiation program", J. Nucl. Mater., 414 , pp. 503–507.

[3] E. D'Agata et al. (2013), "The results of the irradiation experiment MARIOS on americium transmutation", Ann. Nucl. Energy, 62, pp. 40–49.

[4] D. Horlait et al. (2012), "$U_{1-x}Am_xO_{2\pm\delta}$ MABB Fabrication in the Frame of the DIAMINO Irradiation Experiment", Procedia Chem., 7, pp. 485–492.

[5] S. Picart, E. Remy, T. Delahaye (2012), "Method for preparing a porous nuclear fuel", WO2013026851 A1.

[6] E. Remy et al. (2014), "Fabrication of uranium dioxide ceramic pellets with controlled porosity from oxide microspheres", J. Nucl. Mater., 448, pp. 80–86.

[7] Homogeneous versus Heterogeneous Recycling of Transuranics in FastNuclear Reactors, OECD/NEA PUBLISHING, Paris, France, 2012. https://www.oecd-nea.org/science/docs/2012/7077-hvh-recycling-transuranics-fnr.pdf.

[8] J.-M. Gras et al. (2007), "Perspectives on the closed fuel cycle - implications for high-level waste matrices", J. Nucl. Mater., 362, pp. 383–394.

[9] The Generation IV International Forum, (n.d.). https://www.gen-4. org/gif/(accessed 01.12.14)

[10] T. Delahaye et al. (2013), "Application of the UMACS process to highly dense $U_{1-x}Am_xO_{2\pm\delta}$", J. Nucl. Mater., 432, pp. 305–312.

[11] M. Salvatores (2002), "Transmutation: issues, innovative options and perspectives", Prog. Nucl. Energy ,40, pp. 375–402.

[12] R.J.M. Konings et al. (1999), “Transmutation of actinides in inert-matrix fuels: fabrication studies andmodelling of fuel behavior”, J. Nucl. Mater., 274, pp. 84–90.

[13] F. Lebreton et al. (2012), “Fabrication and characterization of americium, neptunium and curium bearing MOX fuels obtained by powder metallurgy process”, J.Nucl. Mater., 420, pp. 213–217.

[14] E. Remy et al. (2012), “Calcined resin microspherepelletization (CRMP): a novel process for sintered metallic oxide pellets”, J.Eur. Ceram. Soc., 32, pp. 3199–3209.

[15] M. Caisso et al. (2014), “Nanostructured gadolinium-doped ceria microsphere synthesis from ion exchange resin: multi-scale in-situ studies of solid solution formation”, J. Solid State Chem., 218, pp. 155–163.

[16] E. Remy (2013), “Etude de la synthèse de sphères d'oxydes d'actinides et/ou de lanthanides et de leur aptitude à la céramisation ”, Thesis of the University of Montpellier.

[17] E. Remy et al. (2014), “Fabrication of uranium-americium mixed oxide pellet from microsphere precursors: Application of CRMP process”, J. Nucl. Mater., 453, pp. 214-219.

[18] K. J. Notz, P. A. Haas and J. H. Shaffer (1978), “The Preparation of HTGR Fissile Fuel Kernels by Uranium-Loading of Ion Exchange Resins”, Radiochim. Acta, 25, pp. 153-160.

[19] D. Prieur et al. (2011), “Self-irradiation effects in dense and tailored porosity $U_{1-y}Am_yO_{2-x}$ (y = 0.10; 0.15) compounds”, J. Nucl. Mater., 411, pp. 15-19.

[20] D. Prieur et al. (2011), “Local Structure and Charge Distribution in Mixed Uranium–Americium Oxides: Effects of Oxygen Potential and Am Content”, Inorg. Chem., 50, pp. 12437-12445.

[21] F.Lebreton et al. (2013), **“**Recent progress on Minor-Actinide-Bearing Oxide Fuel Fabrication at CEA Marcoule”, J. Nucl. Mater., 438, pp. 99 -107.